ELSEVIER

Neuroscience Research 36 (2000) 73–79

NEUROSCIENCE RESEARCH

www.elsevier.com/locate/neures

Directional tuning profiles of motor cortical cells

Bagrat Amirikian [a,b,*], Apostolos P. Georgopulos [a,b,c,d,e]

[a] *Brain Sciences Center, Veterans Affairs Medical Center, 1 Veterans Drive, Minneapolis, MN 55417, USA*
[b] *Department of Neuroscience, University of Minnesota Medical School, Minneapolis, MN 55455, USA*
[c] *Department of Neurology, University of Minnesota Medical School, Minneapolis, MN 55455, USA*
[d] *Department of Psychiatry, University of Minnesota Medical School, Minneapolis, MN 55455, USA*
[e] *Cognitive Sciences Center, University of Minnesota, Minneapolis, MN 55455, USA*

Received 8 October 1999; accepted 25 October 1999

Abstract

The directional tuning profiles of motor cortical cells are commonly described by a cosine tuning function with three adjustable parameters (Georgopoulos, A.P., Kalaska, J.F., Crutcher, M.D., Caminiti, R., Massey, J.T., 1982. On the relations between the direction of two-dimensional (2D) arm movements and cell discharge in primate motor cortex. J. Neurosci. 2, 1527–1537). In this study the variation in the *shape* of the directional tuning profiles among a population of cells recorded from the arm area of the motor cortex of monkeys using movements in 20 directions, every 18°, was examined systematically. This allowed the investigation of tuning functions with extra parameters to capture additional features of the tuning curve (i.e. tuning breadth, symmetry, and modality) and determine an 'optimal' tuning function. These functions provided better fit than the standard cosine one. The optimal function for the large majority of tuned cells was unimodal (84%), and only for a few of them (16%) it was bimodal. Of the unimodal cells, 73% exhibited symmetric and 27% asymmetric shape. The half-width, σ, at the midpoint of optimal tuning curves differed among cells from 30 to 90°, with a median at 56°. This is much narrower than in the standard cosine tuning function with a fixed width of $\sigma = 90°$. It was concluded that motor cortical cells are more sharply tuned than previously thought.

Keywords: Motor cortex; Reaching movement; Tuning shape; Tuning width; Von Mises distribution; Speed modulation

1. Introduction

A relation between the direction of reaching movement, $\boldsymbol{M}$, and cell discharge rate, d, has been established for several brain areas, including the motor cortex, premotor cortex, area 5, cerebellar cortex, and deep cerebellar nuclei (see Georgopoulos, 1991 for a review). This relation can be characterized by a tuning function, $d(\boldsymbol{M})$, the peak of which denotes the 'preferred' direction of the cell, $\boldsymbol{C}$, that is, the direction of movement for which the cell's activity would be highest. The standard tuning function that is used to describe this relation is given by:

$$d(\boldsymbol{M}) = b + k \cos \theta_{\boldsymbol{CM}}, \quad (1)$$

where b and k are cell specific regression coefficients, and $\theta_{\boldsymbol{CM}}$ is the angle between the preferred direction of the cell $\boldsymbol{C}$ and the direction of reaching $\boldsymbol{M}$. This cosine tuning function explains a good percentage of variation in cell activity (see Fig. 1A). It has only three adjustable variables b, k, and $\boldsymbol{C}$ which specify, respectively, the offset of the discharge rate, the depth of the tuning, and the preferred direction of the cell. Although this particular function captures the essential features of directional tuning and does possess the merit of simplicity, it may not be the best one in general. For example, it implies that all cells have the same tuning width and, therefore, does not account for possible variation of this parameter among different cells (see Fig. 1B). The preliminary analysis (Amirikian and Georgopoulos, 1998) indicated that, indeed, breadth of the tuning could vary substantially in a population of directionally tuned cells recorded from the motor cortex of monkeys performing a standard center-out task in two-dimensional (2D) space.

* Corresponding author.
E-mail address: amiri001@maroon.tc.umn.edu (B. Amirikian)

0168-0102/00/$ - see front matter
PII: S0168-0102(99)00112-1

In this study the variation in the *shape* of the tuning profiles among a population of cells recorded from the arm area of the motor cortex of monkeys was examined systematically. Unlike the standard experimental setup (Georgopoulos et al., 1982) in which cell discharge rate is measured for only eight movement directions made 45° apart, tuning profiles obtained for cells used in this study were based on movements made in 20 different directions toward targets located 18° apart on a circle. Such an increase in the number of distinct movement directions allowed one to exploit a family of tuning functions with extra parameters. These functions are able to capture the overall shape and features (e.g. tuning breadth, symmetry, and modality) of the experimentally measured tuning profiles more accurately than a standard cosine tuning function given by Eq. (1).

2. Materials and methods

2.1. Neural and behavioral data

The discharge rates of 73 motor cortical cells used in this study came from single cell recordings performed previously in our laboratory (Georgopoulos and Schwartz, unpublished data). In those experiments monkeys were trained to move a manipulandum in one of 20 instructed directions in 2D space and capture a lighted target to receive a liquid award in a reaction time task (see Georgopoulos et al., 1982). The 20 targets that specified the instructed directions were situated at the circumference of a circle. The directions of the movements made from the center to the peripheral targets covered the whole circle at intervals of 18°. During these experiments the spike activity of single neurons in the arm area of the motor cortex was recorded. The data analyzed consisted of mean discharge rates during the total experimental time, i.e. from the appearance of the target to the end of the movement. The number of trials per instructed direction ranged from 3 to 10. The average speed of the movement toward a target was also calculated.

2.2. Tuning functions

Since movements performed in 2D space are considered, the direction of movement $\boldsymbol{M}$ is uniquely determined by a planar angle, θ, varying in the interval $[-\pi, +\pi]$.

The tuning Eq. (1) can be generalized by substituting the $\cos(x)$ by an arbitrary bell-shaped function $f(x)$ with a period 2π. The tuning equation is then given by:

$$d(\theta) = b + kf(\theta). \tag{2}$$

We considered a family of tuning functions based on:

$$f(\theta) = \exp(\kappa \cos(\theta - \mu)). \tag{3}$$

The form of Eq. (3) is similar (up to a normalization factor) to the von Mises distribution for a directional random variable (von Mises, 1918). In the circular statistics, the von Mises distribution, which is also known as the circular normal distribution, plays a prominent role similar to that of the Gaussian distribution on the line (Mardia, 1972; Batschelet, 1981).

Eqs. (2) and (3) define the *von Mises* tuning function:

$$d(\theta; \boldsymbol{p}_{UM}) = b + k \exp(\kappa \cos(\theta - \mu)), \tag{4}$$

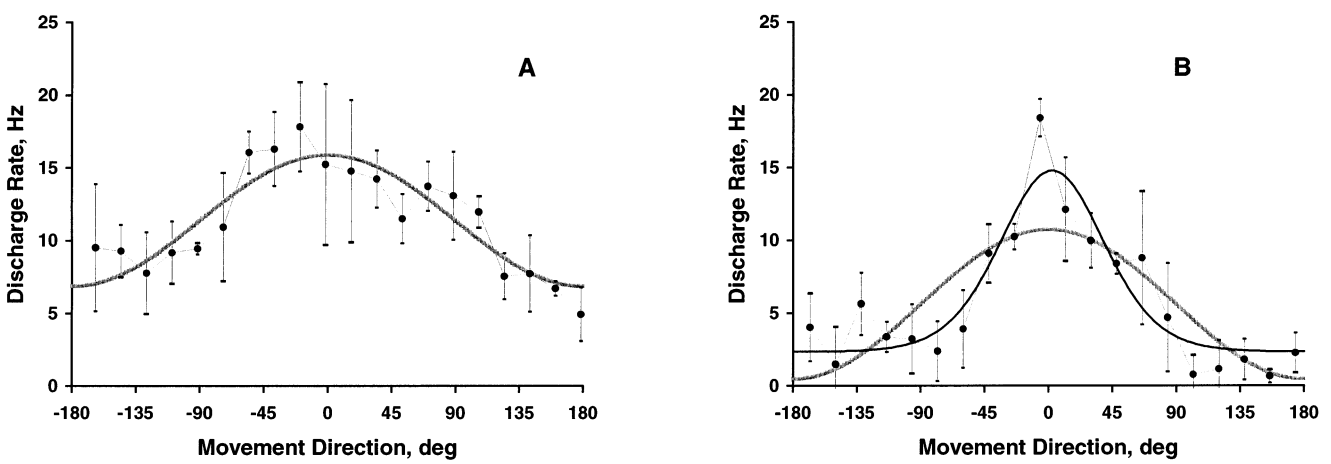

Fig. 1. Breadth of the directional tuning of motor cortical cells. The mean discharge rate (circles), averaged over several trials, is plotted against the direction of movement. Error bars show standard deviation (S.D.) of mean values. The movement direction is relative to the cell's preferred direction. (A) An example of cell whose tuning profile is well explained ($R^2 = 0.81$, $\sigma = 90°$, gray curve) by the standard cosine tuning function (Eq. (1)). The fit of the von Mises function (Eq. (4)) produced a curve ($R^2 = 0.81$, $\sigma = 87°$) that could not be distinguished on this plot from the cosine one. (B) Another cell that has a sharper tuning profile. In this case, the standard cosine function, which has a fixed curve width, yielded a poor fit ($R^2 = 0.64$, gray curve). In contrast, the von Mises function, which is able to adjust its width, produced sharper curve that fits better ($R^2 = 0.83$, $\sigma = 43°$, black curve).

which is unimodal, symmetric, and has a set of adjustable parameters $\boldsymbol{p}_{UM} = \{b, k, \mu, \kappa\}$. The function takes on its maximum value at $\theta = \mu$; hence, μ is the cell's preferred direction. The dimensionless parameter κ ($\kappa > 0$) varies the shape of the function. For $\kappa \ll 1$, the von Mises tuning function degenerates into the standard cosine tuning function, which represents broad tuning. As the value of κ increases, the tuning curve becomes more and more narrow.

In addition to the $d(\theta;\boldsymbol{p}_{UM})$, three other forms of tuning functions were considered:

$$d(\theta; \boldsymbol{p}_{FS}) = b + k \exp[\kappa \cos(\theta - \mu + \eta \sin(\theta - \mu))], \quad (5)$$

$$d(\theta; \boldsymbol{p}_{AS}) = b + k \exp[\kappa \cos(\theta - \mu + \nu \cos(\theta - \mu))], \quad (6)$$

$$d(\theta; \boldsymbol{p}_{BM}) = b + k_1 \exp(\kappa_1 \cos(\theta - \mu_1)) + k_2 \exp(\kappa_2 \cos(\theta - \mu_2)). \quad (7)$$

Like the parent von Mises function $d(\theta; \boldsymbol{p}_{UM})$, the tuning profiles given by Eqs. (5) and (6) with corresponding sets of parameters $\boldsymbol{p}_{FS} = \{b, k, \mu, \kappa, \eta\}$ and $\boldsymbol{p}_{AS} = \{b, k, \mu, \kappa, \nu\}$, respectively, are unimodal. However, each of them has one extra parameter (η, cf. Eq. (5), and ν, cf. Eq. (6)) that gives an additional control over the shape of the tuning profile (for details and illustrations see, for example, Batschelet, 1981). Specifically, depending on the value of the parameter η, the curve $d(\theta;\boldsymbol{p}_{FS})$ is more flat ($-\pi/3 < \eta < 0$) or more sharp ($0 < \eta < \pi/3$) at the mode than von Mises function (Batschelet, 1981). Accordingly, we shall call this tuning function *flat-topped/sharply-peaked*. (Note, for $\eta = 0$ the special case of von Mises tuning function is obtained). In contrast, the parameter ν makes the tuning curve $d(\theta;\boldsymbol{p}_{AS})$ skewed, i.e. asymmetric about its mode. The magnitude of ν is limited to the interval $|\nu| < \pi/6$ and its sign defines the sign of the skewness (Batschelet, 1981). We shall refer to the tuning function $d(\theta; \boldsymbol{p}_{AS})$ as *asymmetric*. For $\nu = 0$ the skewness disappears and, similarly to flat-topped/sharply-peaked function, Eq. (6) becomes identical to the von Mises tuning function.

Finally, the tuning profile $d(\theta; \boldsymbol{p}_{BM})$ given by Eq. (7) is a simple linear combination of two von Mises type functions (cf. Eq. (3)) and, therefore, defines *bimodal* tuning profile with a set of parameters $\boldsymbol{p}_{BM} = \{b, k_1, \mu_1, \kappa_1, k_2, \mu_2, \kappa_2\}$. Note, the parameters that adjust the position (μ_1, μ_2), shape (κ_1, κ_2), and depth of the tuning (k_1, k_2) can be varied for each of the two modes individually.

The general form of tuning function given by Eq. (2) implies that the discharge rate of a cell is modulated only by the direction of movement θ. We extended this description by considering tuning functions that explicitly depend not only on the θ but also on the average speed of movement, v. Two general forms of the *speed modulation* of the discharge rate of a cell were considered: *multiplicative* and *additive*. The former is given by:

$$d(\theta, v; \boldsymbol{p}_{vm}) = b + kvf(\theta), \quad (8)$$

where $f(\theta)$ is the directional modulation of the discharge rate (cf. Eq. (2)). Each of the tuning functions $d(\theta; \boldsymbol{p})$ considered above (Eqs. (4)–(7)) was supplemented by its multiplicative speed offspring function $d(\theta, v;\boldsymbol{p}_{vm})$ given by Eq. (8) and an appropriate $f(\theta)$, which is obtained by subtraction of a bias term b from a corresponding $d(\theta; \boldsymbol{p})$:

$$f(\theta) = d(\theta; \boldsymbol{p}) - b. \quad (9)$$

Note that the number of adjustable parameters $\boldsymbol{p}_{vm}$ in Eq. (8) remained the same as in its correspondent parent tuning function given by Eqs. (4)–(6) or Eq. (7), whereas the number of variables increased by one.

The additive speed offspring, $d(\theta, v; \boldsymbol{p}_{va})$, was obtained simply by adding a linear speed term, αv, to a corresponding parent tuning function $d(\theta; \boldsymbol{p})$:

$$d(\theta, v; \boldsymbol{p}_{va}) = d(\theta; \boldsymbol{p}) + \alpha v \quad (10)$$

As a result, the new set of parameters, $\boldsymbol{p}_{va}$, included one extra parameter α in addition to the set of parameters $\boldsymbol{p}$ of its parent function $d(\theta; \boldsymbol{p})$ given by Eqs. (4)–(6) or Eq. (7).

In conclusion, four tuning functions defined by Eqs. (4)–(7) were supplemented by four multiplicative and four additive speed offspring functions, thus totaling the number of different tuning functions considered per cell to 12. Table 1 summarizes tuning functions and associated number of variables and adjustable parameters.

2.3. Curve fitting

Each of the tuning functions above, $d(\boldsymbol{x}; \boldsymbol{p})$, where $\boldsymbol{x}$ represents either a single variable ($\boldsymbol{x} = \{\theta\}$) or a pair of variables ($\boldsymbol{x} = \{\theta, v\}$), was fitted into experimentally measured discharge rates for individual cells using the least square method. The fitting procedure minimized the following cost function:

$$\Phi(\boldsymbol{p}) = \sum_{i=1}^{N} (d_i - d(\boldsymbol{x}_i; \boldsymbol{p}))^2. \quad (11)$$

For tuning functions that depend only on the direction of movement (i.e. when $\boldsymbol{x} = \{\theta\}$), d_i is the average (across trials) of the mean discharge rate measured for a given cell in the ith direction of movement, and N stands for the total number of different directions. For tuning functions that depend on both movement direction and speed (i.e. when $\boldsymbol{x} = \{\theta, v\}$), d_i is the mean discharge rate in a single trial in the ith direction of movement, whereas N is the total number of recorded trials. The set of parameters $\tilde{\boldsymbol{p}}$ that minimizes $\Phi(\boldsymbol{p})$ is a least square estimate of $\boldsymbol{p}$.

Table 1
The tuning functions, number of their parameters and variables, and the distribution of cells according to their optimal function

Tuning function	Definition	No. parameters	No. variables	No. (%) cells for which the stated function was optimal	No. (%) tuned cells
Von Mises	Eq. (4)	4	1	38 (62.3)	30 (61.2)
Flat/sharp	Eq. (5)	5	1	1 (1.6)	0 (0.0)
Asymmetric	Eq. (6)	5	1	12 (19.7)	11 (22.5)
Bimodal	Eq. (7)	7	1	10 (16.4)	8 (16.3)
Von Mises and SpeedMult	Eqs. (4), (8) and (9)	5	1	0 (0.0)	0 (0.0)
Flat/sharp and SpeedMult	Eqs. (5), (8) and (9)	6	1	0 (0.0)	0 (0.0)
Asymmetric and SpeedMult	Eqs. (6), (8) and (9)	6	1	0 (0.0)	0 (0.0)
Bimodal and SpeedMult	Eqs. (7)–(9)	8	1	0 (0.0)	0 (0.0)
Von Mises and SpeedAdd	Eqs. (4) and (10)	5	2	0 (0.0)	0 (0.0)
Flat/sharp and SpeedAdd	Eqs. (5) and (10)	6	2	0 (0.0)	0 (0.0)
Asymmetric and SpeedAdd	Eqs. (6) and (10)	6	2	0 (0.0)	0 (0.0)
Bimodal and SpeedAdd	Eqs. (7) and (10)	8	2	0 (0.0)	0 (0.0)
Total				61 (100.0)	49 (100.0)

The goodness of fit was assessed by computing the coefficient of determination, R^2, defined in a following way (Goldberger, 1964; Kvalseth, 1985):

$$R^2 = 1 - \frac{\sum_{i=1}^{N} (d_i - d(\boldsymbol{x}_i; \tilde{\boldsymbol{p}}))^2}{\sum_{i=1}^{N} (d_i - \bar{d})^2}, \quad (12)$$

where $\bar{d}$ denotes the arithmetic mean of d_i. The value of R^2 may be interpreted as the proportion of the total variation of discharge rate d_i (about its mean $\bar{d}$) that is explained by the fitted tuning function $d(\boldsymbol{x}; \tilde{\boldsymbol{p}})$. Note, $R^2 \leq 1$ and the minimization of $\Phi(\boldsymbol{p})$ is equivalent to maximization of R^2, where $R^2 = 1$ corresponds to perfect fit.

A nonlinear regression algorithm implemented in the IMSL Statistical Library Package, Visual Numerics, was used to find the least square estimate of the parameters for the tuning functions given by Eqs. (4)–(7) and their multiplicative and additive speed offspring defined by Eqs. (8)–(10), respectively. The linear fit to the standard cosine tuning (Eq. (1)) was done as it is described in Georgopoulos et al. (1982).

2.4. Tuning curve width

One of the main goals of this work was to examine the variation in the breadth of the directional tuning in motor cortical cells. To compare the breadth of fitted curves in a systematic way one needs a quantitative measure that would characterize the tuning curve width consistently, regardless of which particular tuning function is employed. We used the half-width, σ, at the midpoint of the tuning curve as such measure.

3. Results

We analysed data from 61 (out of the total 73) cells that showed a significant effect of the direction of movement on cell discharge rate (ANOVA, $P < 0.05$; Zar, 1984). Fig. 1(A) shows a plot of the discharge rate of a cell as a function of the movement direction. This relation is well explained ($R^2 = 0.81$) by the standard cosine tuning function (Eq. (1)). The discharge rates of another cell are shown in Fig. 1(B). Despite the fact that this cell also demonstrates features of the directional tuning, the cosine function produced a poor fit ($R^2 = 0.64$) in this case (Fig. 1B, gray curve). The reason for this is the fixed width ($\sigma = 90°$, see Section 2 for the definition of σ) of the cosine tuning function.

To examine systematically the variations in the shape of the tuning profiles, we employed a family of tuning functions given by Eqs. (4)–(7). The von Mises (Eq. (4)) and flat-topped/sharply-peaked (Eq. (5)) functions are unimodal, symmetric, and suitable to describe a set of tuning profiles that show substantial variations in the breadth as well as overall shape. For example, the fit of the von Mises function, which has a parameter κ that varies the breadth of the curve (cf. Eq. (4)), to the same data shown in Fig. 1(B) produced better results (Fig. 1B, black curve; $R^2 = 0.83$) as compared to the cosine

fit. The width of the von Mises tuning curve in this case is $\sigma = 43°$.

The tuning function given by Eq. (6) produces unimodal but asymmetric curves whereas Eq. (7) defines bimodal tuning profiles. Fig. 2 shows an example of two cells the discharge rates of which are well explained by the asymmetric (Fig. 2A, $R^2 = 0.85$, cf. $R^2 = 0.71$ for the von Mises function, which is symmetric) and bimodal (Fig. 2B, $R^2 = 0.97$, cf. $R^2 = 0.61$ for the von Mises function that captures only the main mode) tuning profiles.

The four tuning functions given by Eqs. (4)–(7) were fitted into the discharge rates of 61 cells under study and the corresponding R^2 values were computed. These functions imply that the discharge rate of a cell, $d(\theta; \boldsymbol{p})$, is modulated only by the direction of movement θ. We broadened this description and considered tuning functions that explicitly depend not only on the θ but also on the average speed of movement v. Namely, each of the tuning functions $d(\theta; \boldsymbol{p})$ (Eqs. (4)–(7)) was supplemented by two offspring functions (Eqs. (8) and (10)) of which $d(\theta, v; \boldsymbol{p}_{vm})$ includes multiplicative effect of speed whereas the other, $d(\theta, v; \boldsymbol{p}_{va})$, includes an additive speed component (see Section 2). Therefore, in total, 12 fitted curves and 12 corresponding to them R^2s were computed per each cell.

As it was expected, the tuning functions that have more adjustable parameters provide, in general, better fit (i.e. larger R^2). For example, flat-topped/sharply-peaked, asymmetric, and bimodal tuning functions all have additional parameters as compared to their parent von Mises function (cf. Table 1 and Eqs. (4)–(7)). By setting these extra parameters to zero, each of these tuning functions reduces to the special case of the von Mises function. Therefore, flat-topped/sharply-peaked, asymmetric, and bimodal tuning functions will always fit to data better than the von Mises function. This improvement, however, is achieved by sacrificing the simplicity of the original function and selecting a new one that has relatively more complex functional form. Which function, the simple or complex one, is better? This question is well known in the regression analysis. Unfortunately, even in the linear case there is no unique statistical procedure for selecting the 'best' regression equation (Draper and Smith, 1981). Several approaches that were proposed do not necessarily lead to the same results (Draper and Smith, 1981). Therefore, a great deal of personal judgement is usually exercised.

In this work a simple intuitive approach was used for selecting the optimal tuning equation. It is based on a trade-off between the R^2 and the 'complexity', C, of the underlying tuning function. Specifically, each tuning function fitted to the discharge rates of a given cell is assigned a score, s, given by:

$$s_f = R_f^2 - \lambda C_f. \tag{13}$$

Here, λ is a constant; index f is shown to emphasize that variables depend on the type of a tuning function for which the score is computed. The complexity C_f was measured simply as a sum of the number of adjustable parameters, n_f, and number of independent variables, n_x, of the tuning function in consideration: $C_f = n_f + n_x$. The constant λ then has a simple meaning of a penalty (in the units of R^2) that is paid for a single adjustable parameter or a variable of the tuning function. The more parameters and/or variables the tuning function has, the more it is penalized (cf. Eq. (13)). On the other hand, the increase in the number of parameters, in general, leads to the better fit (i.e. larger R^2) and, therefore, the greater reward.

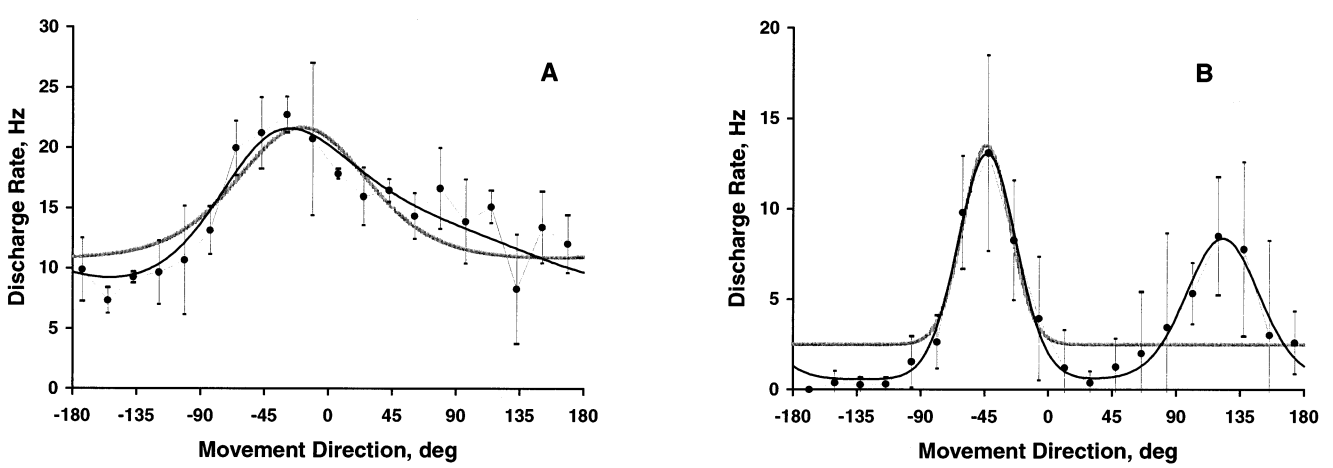

Fig. 2. Shape of the directional tuning. The plots are represented in the same format as in Fig. 1. (A) Asymmetric tuning profile. In this example, the tuning function (Eq. (6)), which may adopt asymmetric shapes, provided considerably better fit ($R^2 = 0.85$, black curve) as opposed to the symmetric von Mises function ($R^2 = 0.71$, gray curve). (B) Bimodal tuning profile. A linear combination of two von Mises functions (Eq. (7)) produced a curve that perfectly captured bimodality of this cell ($R^2 = 0.97$, black curve). The unimodal von Mises function (Eq. (4)) explained only the main mode ($R^2 = 0.61$, gray curve).

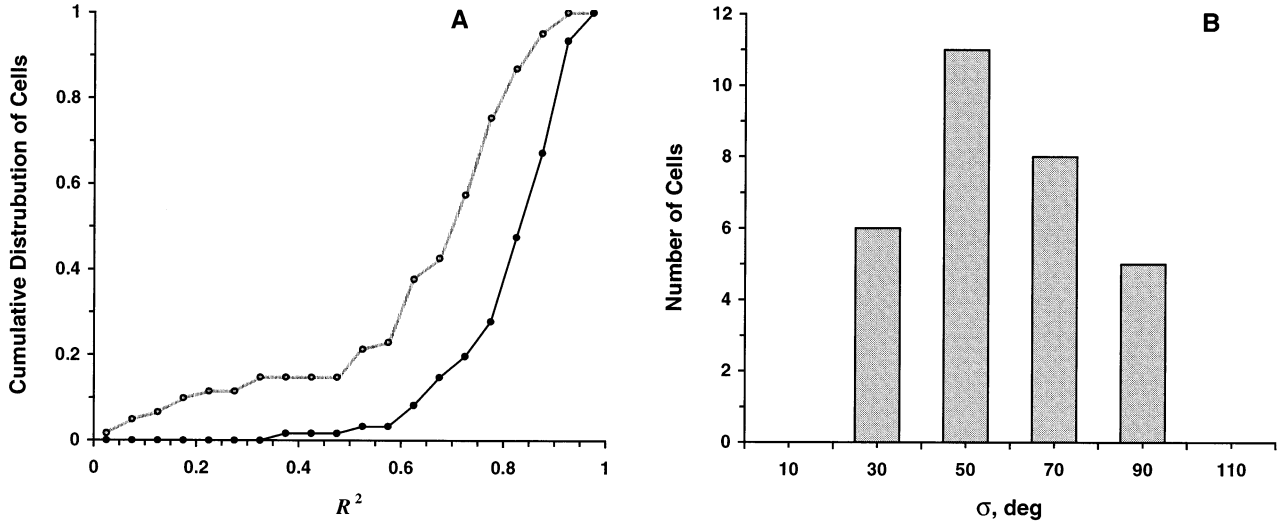

Fig. 3. (A) The cumulative distribution of the R^2 values of the optimal (black curve) and standard cosine (gray curve) tuning functions computed for 61 cells. The computed R^2 values for individual cells are grouped into bins of 0.05 width. (B). The distribution of the curve width σ among a population of 30 cells for which the von Mises function was the optimal and the fit resulted in $R^2 > 0.75$. The σ values of individual cells are grouped into 20° wide bins.

The score s_f was computed for each tuning function fitted to the discharge rates of a given cell. The function that received the highest score was declared as the 'optimal'. This procedure was applied to the all cells and thus classified each of them in accordance with its own optimal tuning function. The results of such a consideration for $\lambda = 0.05$ (equivalent to 5% if R^2 is measured in percentage) is presented in Table 1.

Fig. 3(A) shows the cumulative distribution of the R^2 computed for the optimal (black curve) and standard cosine (gray curve) tuning functions. It is seen that the optimal tuning functions consistently improve the fit (cf. Fig. 3A, the black curve is steeper than the gray one and substantially shifted to larger R^2 values; Kolmogorov–Smirnov test, $P < 10^{-7}$) as compared to the cosine function. The increase in the R^2 value, ΔR^2, for individual cells varied in the interval $0 < \Delta R^2 < 0.91$ and in average $\Delta R^2 = 0.18$.

Despite the fact that the optimal tuning functions provide better explanation of the experimental data, still there is a fraction of cells with relatively low R^2 values. To cut-off these cells from further analysis, a cell was considered 'tuned' to its optimal function only if its corresponding $R^2 > 0.75$ (Moran and Schwartz, 1999). The resultant distribution of the tuned cells across the family of functions considered in this study is shown in Table 1. It is seen that none of the speed offspring tuning functions were selected as an optimal one for the cells analyzed in this study.

Next, the question of how the width of individual tuning curves varied among a population of 30 cells with symmetric tuning profiles was examined. Fig. 3(B) shows the distribution of the parameter σ, which characterizes the breadth of the tuning, for these cells. It is seen that σ varies in a wide range, from 30 to 90°, with a median at 56°. This is in a sharp contrast to the case of the standard cosine tuning function in which all cells would have the same tuning curve width $\sigma = 90°$ (cf. Fig. 1).

We found that the average speed of movement has a negligible effect on the shape of the tuning profiles.

4. Discussion

The main point of this paper is that the shape of directional tuning profiles exhibited by motor cortical neurons varies from cell to cell substantially, and more than previously thought. This observation became possible due to the changes, for this particular study, in the experimental setup that considerably increased the number of distinct movement directions at which cell discharge rates are measured. It is this qualitative improvement in the experimental accuracy that justified exploitation of tuning functions with more parameters than the standard cosine one suggested in Georgopoulos et al. (1982).

The tuning functions used in this study were defined in such way that, when their adjustable parameters are set to appropriate values, they could be reduced to the special case of von Mises function (Eq. (4)). For $\kappa \ll 1$, the latter, in turn, degenerates into the standard cosine tuning given by Eq. (1). This means that, if cells are truly cosine tuned, the least square fit of the underlying functions will produce tuning curves with a shape very similar to the standard cosine function, irrespective of the extra parameters that these functions posses. Indeed, for some neurons, the shapes of von Mises func-

tions, which turned to be the optimal tuning functions for these cells, are almost indistinguishable from the standard cosine profile (e.g. see Fig. 1A). The width, σ, of a von Mises curve in this case is close to 90°, which is the width of the standard cosine function. However, only five such cells (i.e. 10% of 49 cells considered tuned) were found (cf. histogram at $\sigma = 90°$, Fig. 3B). In fact, the tuning profiles of 25 other neurons (51%), for which the optimal function was the von Mises, were considerably narrower than the cosine. The distribution of σ is bell-shaped (cf. Fig. 3B) with a mode at 59°.

The differences in the tuning shapes could be not only quantitative but, in some cases, also qualitative. Specifically, we found that the optimal tuning functions for 11 cells (23%) are asymmetric (e.g. Fig. 2A), whereas for eight other cells (16%) they are bimodal (e.g. Fig. 2B). Interestingly, none of the cells were characterized by the flat-topped/sharply-peaked tuning function.

Analyses of the time course of cell activity (Ashe and Georgopoulos, 1994; Moran and Schwartz, 1999) has shown that the *time varying discharge rates* of individual cells represent not only the direction but also the *time varying speed* of reaching movement. It is important to realize, however, that a specific relation between the instantaneous values of some variables does not necessarily hold for their average, over time, values. Specifically, the relation between the time varying discharge rate and speed (Ashe and Georgopoulos, 1994; Moran and Schwartz, 1999) may not be present for their *time-averaged* values, i.e. the mean discharge rate and average movement speed, which, by definition, do not contain information about the detailed time course of these variables. Indeed, we found that the tuning functions that account for the average speed either multiplicatively or additively did not provide better fit, i.e. did not substantially increase the R^2 value, as compared to their parent functions. As a result the scores (Eq. (13)) computed for the speed offspring functions were small and none of them were selected as an optimal one.

Finally, the finding that most of the cells have much narrower tuning profiles than previously thought may have implications for neural network modeling of motor cortical cells. Moreover, we believed that some previous modeling studies that are heavily based on the assumption of the cosine shape of the directional tuning should be revisited and their conclusions, perhaps, should be re-evaluated.

Acknowledgements

Supported by USPHS grants PSMH48185 and NS17413, the Department of Veterans Affairs, and the American Legion Brain Sciences Chair.

References

Amirikian, B., Georgopoulos, A.P., 1998. Directional tuning functions of motor cortical cells. Soc. Neurosci. Abstr. 24, 404.

Ashe, J., Georgopoulos, A.P., 1994. Movement parameters and neural activity in motor cortex and area 5. Cereb. Cortex 6, 590–600.

Batschelet, E., 1981. Circular Statistics in Biology. Academic Press, London.

Draper, N.R., Smith, H., 1981. Applied Regression Analysis. Wiley, New York.

Georgopoulos, A.P., 1991. Higher order motor control. Annu. Rev. Neurosci. 14, 361–377.

Georgopoulos, A.P., Kalaska, J.F., Crutcher, M.D., Caminiti, R., Massey, J.T., 1982. On the relations between the direction of two-dimensional arm movements and cell discharge in primate motor cortex. J. Neurosci. 2, 1527–1537.

Goldberger, A.S., 1964. Econometric Theory. Wiley, New York.

Kvalseth, O., 1985. Cautionary note about R^2. Am. Stat. 39, 279–285.

Mardia, K.V., 1972. Statistics of Directional Data. Academic Press, London.

Moran, D.W., Schwartz, A.B., 1999. Motor cortical representation of speed and direction during reaching. J. Neurophysiol. 82, 2676–2692.

von Mises, R., 1918. Über die 'Ganzzahligkeit' der Atomgewicht und verwandte Fragen. Phys. Z. 19, 490–500.

Zar, J.H., 1984. Biostatistical Analysis. Prentice-Hall, Englewood Cliffs, NJ.